The International Journal of Cardiovascular Imaging (2019) 35:1971–1978
https://doi.org/10.1007/s10554-019-01651-4

ORIGINAL PAPER

Neointimal tissue characterization after implantation of drug-eluting stents by optical coherence tomography: quantitative analysis of optical density

Setsu Nishino[1,2] · Masashi Sakuma[1] · Tomoaki Kanaya[1] · Takahisa Nasuno[1] · Michiaki Tokura[1] · Shigeru Toyoda[1] · Shichiro Abe[1] · Daisuke Nakamura[2] · Kentaro Tanaka[2] · Guiherme F. Attizzani[2] · Hiram G. Bezerra[2] · Marco A. Costa[2] · Teruo Inoue[1]

Received: 20 February 2019 / Accepted: 13 June 2019 / Published online: 19 June 2019

Abstract

Normalized optical density (NOD) measured by optical coherence tomography represents neointimal maturity after coronary stent implantation and is correlated with morphologic information provided by both light and electron microscopy. We aimed to test the hypothesis that even second generation drug-eluting stents (DESs) are problematic in terms of neointimal maturity. We implanted bare-metal stents (BMS: n = 14), everolimus-eluting stents (EESs: n = 15) or zotarolimus-eluting stents (ZESs: n = 12) at 41 sites in 32 patients with stable coronary artery disease. OCT was performed at up to 12 months of follow-up, and the average optical density of neointima covering struts was evaluated. NOD was calculated as the optical density of stent-strut covering tissue divided by the optical density of the struts. We also measured circulating CD34+/CD133+/CD45low cells, and serum levels of stromal cell-derived factor (SDF)-1, interleukin (IL)-8 and matrix metalloproteinase (MMP)-9 at baseline and follow-up. NOD was lower in the EES (0.70 ± 0.06) group than in the BMS (0.76 ± 0.07, $P < 0.05$) and ZES (0.76 ± 0.06, $P < 0.05$) groups. The mean neointimal area ($R = 0.33$, $P < 0.05$) and mean neointimal thickness ($R = 0.37$, $P < 0.05$) were correlated with NOD. Although NOD was not correlated with percent changes in circulating endothelial progenitor cells, and the levels of SDF-1 and IL-8, it was negatively correlated with the change in MMP-9 level ($R = -0.51$, $P < 0.01$). Neointimal maturity might be lower at EES sites than BMS or ZES sites. This might lead to impaired neointimal tissue growth and matrix degradation. These results suggest a specific pathophysiology after DES implantation.

Keywords Optical coherence tomography · Drug-eluting stent · Vascular injury · Re-endothelialization · Neointimal maturity

Introduction

Drug eluting stents (DESs) have substantially reduced angiographic and clinical restenosis rates across broad lesion and patient subsets compared with bare metal stents (BMSs). However, current DESs do not necessarily benefit all patients with coronary artery disease (CAD). A unique issue beyond restenosis after DES implantation is the potential for impairment of re-endothelialization, which leads to lack of neointima formation and neointimal coverage over the stent struts. Exposed stent struts potentially cause stent thrombosis, which could happen even very late after stent implantation [1–5]. In addition, impaired re-endothelialization delays wound healing and causes a relapse of inflammation at the stent-injured sites when the anti-inflammatory effects of the drugs coated on DESs disappear [6], potentially inhibiting the formation of neointima. In the process of wound healing after stent implantation, CD34-positive cells are mobilized into the circulation and are positively correlated with an increased risk of restenosis [7].

Optical coherence tomography (OCT) assessment of stent-vessel interaction has been used in vivo as a surrogate endpoint to evaluate the healing process after DES implantation. The pixel intensity (optical density) of the

✉ Setsu Nishino
setsu@dokkyomed.ac.jp

[1] Department of Cardiovascular Medicine, Dokkyo Medical University, Mibu, Tochigi, Japan

[2] Cardiovascular Imaging Core Laboratory, Harrington Heart and Vascular Institute, University Hospitals Cleveland Medical Center, Case Western Reserve University, Cleveland, OH, USA

tissue covering the stent struts based on OCT imaging, normalized for optical density of the stent struts, provides information about neointimal maturity [8–11].

First-generation DESs, such as sirolimus-eluting stents (SES) and paclitaxel-eluting stents (PESs), were followed by the development of second-generation DESs, such as zotarolimus-eluting stents (ZESs) and everolimus-eluting stent (EESs), and these newer DESs are now mainly used in clinical practice. Although these new-generation DESs have been suggested to be better in terms of local wound healing in the stent-injured vessel wall sites compared with first-generation DESs, this has not yet been completely established.

This study was designed to compare neointimal maturity after BMS, ZES and EES placement, and to investigate the pathophysiological mechanism of neointimal maturity and its role in vascular healing after stent implantation.

Methods

Study design

The subjects included 32 consecutive patients (22 men and 10 women, aged 70 ± 9 years) with stable coronary artery disease who underwent elective coronary stent implantation for organic lesions in a single coronary artery using a BMS (n = 13), ZES (n = 7) or EES (n = 12). When multiple stenting was required in a single patient, the same type of stents were implanted. Stent choice among BMSs, ZESs or EESs was based upon each operator's decision. All of the patients received dual anti-platelet therapy with 81 mg of aspirin and 75 mg clopidogrel at least until the follow-up coronary angiography. Follow-up coronary angiography was recommended at 12 months after stent implantation, but was performed earlier if necessary based on clinical indications. At the time of follow-up coronary angiography, we assessed re-endothelialization and neointimal growth at each of the stented sites using OCT imaging. Also, peripheral blood samples were collected from all patients at baseline before stenting and at the follow-up study. The blood samples were immediately collected into tubes containing ethylene diaminetetraacetate (EDTA) and plain tubes. We measured the number of circulating CD34+/CD13+/CD45low progenitor cells using the blood in the EDTA tubes, and serum level of biomarkers such as stromal cell-derived factor (SDF)-1α, interleukin (IL)-8, and matrix metalloproteinase (MMP)-9 using the blood in the plain tubes. All patients provided written informed consent. The study protocol was approved by the local institutional review board in Dokkyo Medical University (Mibu, Tochigi, Japan) and complied with the Declaration of Helsinki.

Optical coherence tomography imaging and analysis

At the time of follow-up coronary angiography, OCT was performed using a frequency-domain system (C7-XR FD-OCT Intravascular Imaging System; St. Jude Medical, St. Paul MN) after administration of intracoronary nitroglycerin. Two independent readers from the Cardiovascular Imaging Core Laboratory (Cardiovascular Imaging Core Laboratory, Harrington Heart & Vascular Institute, University Hospitals, Cleveland Medical Center, OH), blinded to patient information, performed quantitative and qualitative OCT analyses using dedicated software (Off-line Review Software, version E.0.2, St. Jude Medical). All cross-sectional images were initially screened for quality assessment and excluded if any frame had a stent that was out of the screen or if the image had poor quality caused by residual blood, artifact or reverberation [12]. For morphometric analysis, standard definitions of cross-sectional area and volume measurements were applied, as previously reported [12]. Strut-level analysis was performed using all analyzable frames along the stented segment. Stent strut coverage and malapposition were defined and measured as described previously [13, 14].

Optical density of stent strut covering tissue

Based on OCT imaging properties, we evaluated the pixel intensity (optical density) of stent strut covering tissue localized on the inner side of the struts, and normalized the value for the optical density of the stent struts (Fig. 1). The values of optical density were obtained automatically using proprietary computer-assisted analysis software (St. Jude Medical). A previous study showed that normalized optical density (NOD), defined as the optical density of stent strut covering tissue divided by the optical density of the stent struts, was significantly correlated with morphologic information provided by both light and electron microscopy [8]. NOD

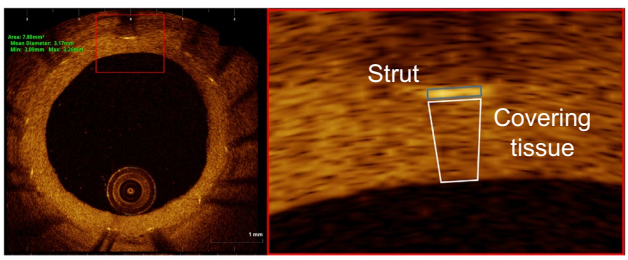

Normalized optical density (NOD)

= Mean intensity of covering tissue / mean intensity of strut

Fig. 1 Calculation of normalized optical density (NOD)

was measured on all struts in the cross-section every 0.6 mm in the same frames used to perform quantitative analysis. A region of interest was manually drawn by two experienced OCT analysts, and the results were reviewed by a third analyst. The average of all the measured struts was calculated as a marker of neointimal maturity [9–11].

Biomarker measurements

We measured circulating CD34+/CD133+/CD45low cells, which included endothelial progenitor cells, using flow cytometry based on a previously described method [7, 15, 16] with minor modifications. The reagent mixture included a peridinine chlorophil protein (PerCP)-conjugated anti-CD45 antibody (Becton Dickinson), a fluorescein isothiocyanate (FITC)-conjugated anti-CD34 antibody (Becton Dickinson) and a phycoerythrin (PE)-conjugated anti-CD133 antibody (Miltennyi Biotec). Isotype controls were used as negative controls based on the species and immunoglobulin (Ig) G control antibodies (IgG1 isotype control; Becton Dickinson). Flow cytometric analysis was performed using the FACS Calibur laser flow cytometer (Becton Dickinson) according to the manufacturer's instructions. The absolute number of CD34+/CD133+/CD45low cells per milliliter was calculated based on the cells-to-the white blood cell count ratio. To minimize any methodological variations, each sample was analyzed with two independent experiments, and the mean value was calculated.

In this study, we also measured serum levels of stromal cell-derived factor (SDF)-1α, interleukin (IL)-8, and matrix metalloproteinase (MMP)-9, using an enzyme-linked immunosorbent assay (ELISA). We used commercially available ELISA kits (Quantikine ELISA kits; R&D Systems) to measure SDF-1α (Human CXCL12/SDF-1α Immunoassay), IL-8 (Human CXCL8/IL-8 Immunoassay), and MMP-9 (Human MMP-9 Immunoassay). The procedure was performed according to the manufacturer's instructions. Each sample was assayed in duplicate for standards and controls; and high, medium and low standards were included in each run. The colorimetric reactions were read on an automatic microplate reader set to 450 nm. The concentration of each biomarker in a sample was determined by interpolation from a standard curve.

Statistical analyses

The normality of the distributions of variables was assessed using the Kolmogorov–Smirnov test with Lilliefors' correction. If the distributions were not parametric, the data were transformed into logarithmic values. Data are presented as means ± standard deviations (SD). Differences among the three groups were assessed with a chi-square test for categorical variables and with an analysis of variance (ANOVA) followed by Scheffe's post hoc test for continuous variables. Intra-group comparisons between baseline and follow-up were performed using a paired t-test for normally distributed data and a Wilcoxon Rank Sum test for data with a skewed distribution. Spearman's correlation analysis was used to assess the relationship between two parameters. $P < 0.05$ was considered significant.

Results

Baseline characteristics were compared among each patient group that had BMS, ZES or EES implantation (Table 1). There were no significant differences in age, gender, coronary risk factors or medications among the three groups. The follow-up times were also similar in the BMS, ZES and EES groups (8.3 ± 3.0, 9.7 ± 2.1 and 9.6 ± 2.1 months, respectively).

In the 32 study patients, a total of 41 stents (BMS: n = 14, ZES: n = 12, EES: n = 15) were implanted. The conventional OCT image analysis data for each stent site are shown in Table 2. The mean neointimal area (BMS vs. EES, $P < 0.001$; ZES vs. EES, $P < 0.001$), neointimal volume (BMS vs. EES, $P < 0.001$; ZES vs. EES, $P < 0.05$) and mean neointimal thickness (BMS vs. EES, $P < 0.001$; ZES vs. EES, $P < 0.01$) were lower in the EES group than the BMS and ZES groups. The percentage of uncovered struts was higher in the EES group than the BMS ($P < 0.05$) and ZES ($P < 0.01$) groups. The percentage of malapposed struts was also higher in the EES group than the BMS ($P < 0.05$) and ZES ($P < 0.05$) groups. Furthermore, the NOD was lower in

Table 1 Baseline characteristics

	BMS (n = 13)	ZES (n = 7)	EES (n = 12)
Age: years	69 ± 11	72 ± 6	70 ± 8
Male gender [n (%)]	10 (77)	5 (71)	6 (46)
Coronary risk factors [n (%)]			
Hypertension	11 (85)	6 (87)	12 (92)
Diabetes	5 (39)	2 (29)	7 (54)
Dyslipidemia	9 (69)	6 (86)	11 (85)
Current smoking	7 (54)	4 (57)	7 (54)
Medications [n (%)]			
Statins	9 (69)	5 (71)	12 (92)
ACEIs/ARBs	10 (77)	5 (71)	12 (92)
Antidiabetic agents	3 (23)	2 (29)	5 (39)
Follow-up interval (months)	8.3 ± 3.0	9.7 ± 2.1	9.6 ± 2.1

BMS bare metal stent, *ZES* zotarolimus-eluting stent, *EES* everolimus-eluting stent, *ACEI* angiotensin converting enzyme inhibitors, *ARB* angiotensin receptor blocker

Table 2 Conventional OCT image analysis data

	BMS (n = 14)	ZES (n = 12)	EES (n = 15)
Mean reference diameter (mm)	2.83 ± 0.38	0.59 ± 0.26	0.41 ± 0.46
Mean reference area (mm^2)	6.45 ± 1.75	5.41 ± 1.10	4.79 ± 1.83
Mean stent area (mm^2)	8.80 ± 2.91	8.22 ± 1.57	6.53 ± 2.06
Mean luminal area (mm^2)	2.49 ± 0.53	3.88 ± 1.19	4.20 ± 1.99
Mean neointimal area (mm^2)	3.61 ± 1.55	2.46 ± 0.86	0.93 ± 0.59**,†††
Mean neointimal thickness (μm)	401 ± 151	265 ± 75	119 ± 93**
Uncovered struts (%)	0.91 ± 1.56	0.32 ± 0.57	11.0 ± 15.3*,††
Malapposed struts (%)	0.05 ± 0.19	0.06 ± 0.20	1.34 ± 2.85*,†
NOD	0.76 ± 0.07	0.76 ± 0.06	0.70 ± 0.06*,†

BMS bare metal stent, *ZES* zotarolimus-eluting stent, *EES* everolimus-eluting stent, *OCT* optical coherence tomography, *NOD* normalized optical density

*P < 0.05, **P < 0.001 versus BMS

†P < 0.05, ††P < 0.01, †††P < 0.001 versus ZES

the EES group than the BMS (P < 0.05) and ZES (P < 0.05) groups (Table 2).

In 28 of the 32 study patients, circulating CD34+/CD133+/CD45low cells and levels of SDF-1α, IL-8 and MMP-9 were measured both at baseline before stenting and at the time of follow-up. There were no significant differences in the values of these biomarkers among the three groups at either baseline or follow-up. The percent change in the value ([follow-up value − baseline value] × 100/baseline value) of CD34+/CD133+/CD45low cells was less in the EES group than the BMS group (P < 0.05). However, there were no significant differences in the percent changes in the levels of SDF-1α, IL-8 and MMP-9 among the three groups (Table 3).

The mean neointimal area (R = 0.33, P < 0.05) and mean neointimal thickness (R = 0.37, P < 0.05) were correlated with the NOD value (Fig. 2). The NOD value was not correlated with each of the percent changes in CD34+/CD133+/CD45low cells (R = 0.16), SDF-1α level (R = 0.10) and IL-8 level (R = 0.32), but it was negatively correlated with the percent change in MMP-9 level (R = −0.51, P < 0.01) (Fig. 3).

Table 3 Comparison of circulating biomarkers among the BMS, ZES and EES groups

	BMS (n = 13)	ZES (n = 6)	EES (n = 9)
CD34+ /CD133+ / CD45low cells			
Baseline	262 ± 120	326 ± 240	342 ± 88
Follow-up	432 ± 251	323 ± 226	336 ± 108
% Change	69 ± 67	16 ± 77	−1 ± 25*
SDF-1α			
Baseline	2109 ± 670	1859 ± 713	1878 ± 749
Follow-up	2220 ± 799	1677 ± 387	2098 ± 939
% Change	27 ± 82	0 ± 34	16 ± 52
IL-8			
Baseline	203 ± 72	173 ± 29	191 ± 25
Follow-up	196 ± 77	183 ± 47	213 ± 62
% Change	1 ± 30	7 ± 30	13 ± 35
MMP-9			
Baseline	3220 ± 1797	2655 ± 748	2481 ± 906
Follow-up	2341 ± 760	2331 ± 729	2600 ± 1547
% Change	−17 ± 28	−11 ± 24	11 ± 53

SDF-1α stromal cell-derived factor-1α, *IL-8* interleukin-8, *MMP-9* matrix metalloproteinase-9

*P < 0.05 versus BMS

Discussion

In the present study, we demonstrated that the OCT-based NOD as well as neointimal growth and neointimal strut coverage were lower at EES sites than at BMS and ZES sites, and that the mean neointimal area and mean neointimal thickness were correlated with the NOD over the entire length of the stented segment. Representative OCT cross-sectional images with NOD analysis for each stent are shown in Fig. 4. The results suggest that neointima might be immature at EES sites, compared with BMS and ZES sites, and that neointimal maturity might lead to neointimal tissue growth.

Generational advances in DES technology have resulted in reduced rates of target lesion revascularization across broad patient and lesion subsets with improved safety with respect to stent thrombosis. However, concerns over incomplete stent healing even with second-generation DESs persist because the annual rate of target lesion failure still remains at 2–4%, which is similar to the rates observed after implantation of BMSs or first-generation DESs [17]. From a vascular biology perspective, there is consensus that late-lumen

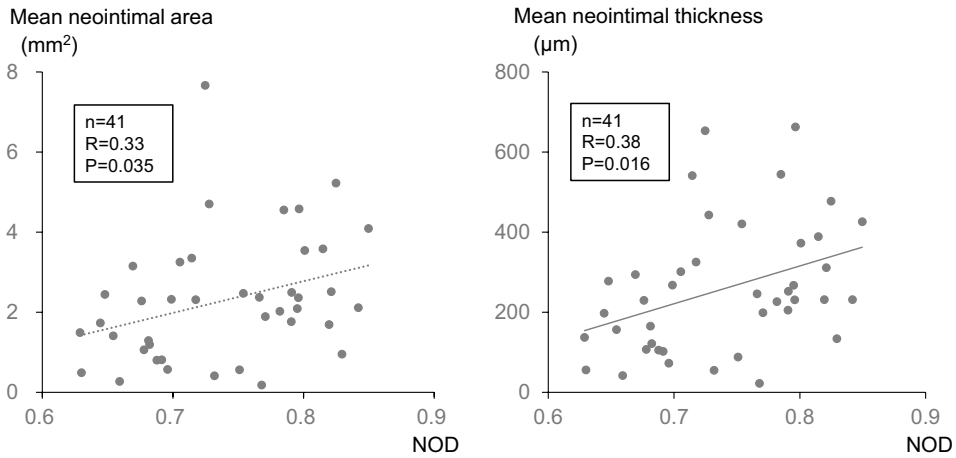

Fig. 2 Relationship between NOD and neointimal growth. The mean neointimal area and mean neointimal thickness were correlated with the NOD. *NOD* normalized optical density

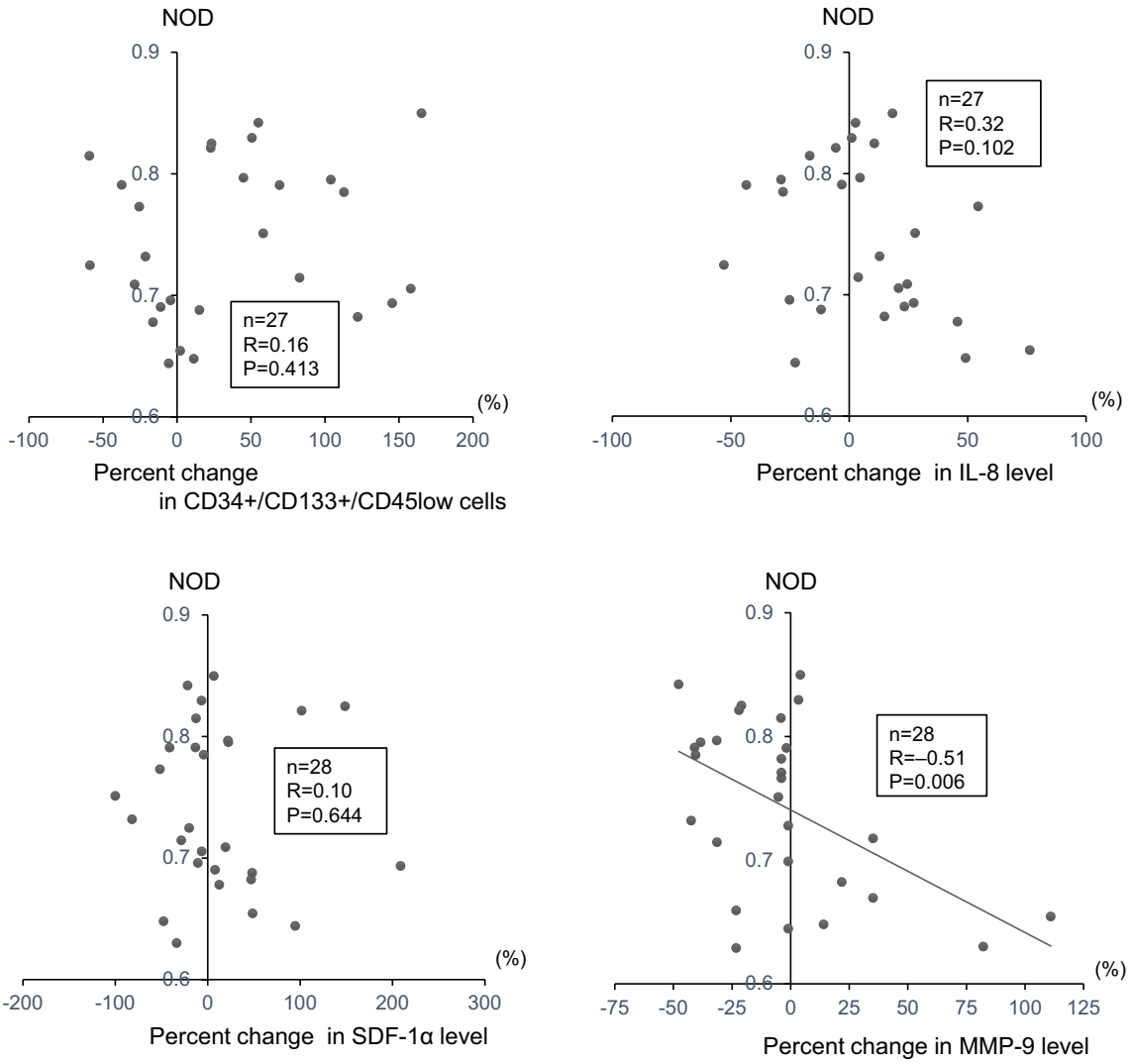

Fig. 3 Relationship between NOD and percent change in biomarkers ([value at follow-up − baseline value] × 100/baseline value). NOD was not correlated with changes in CD34+ CD133+ CD45low cells or SDF-1α and IL-8 levels, but was negatively correlated with the change in MMP-9 level. *SDF* stromal cell-derived factor, *IL* interleukin, *MMP* matrix metalloproteinase

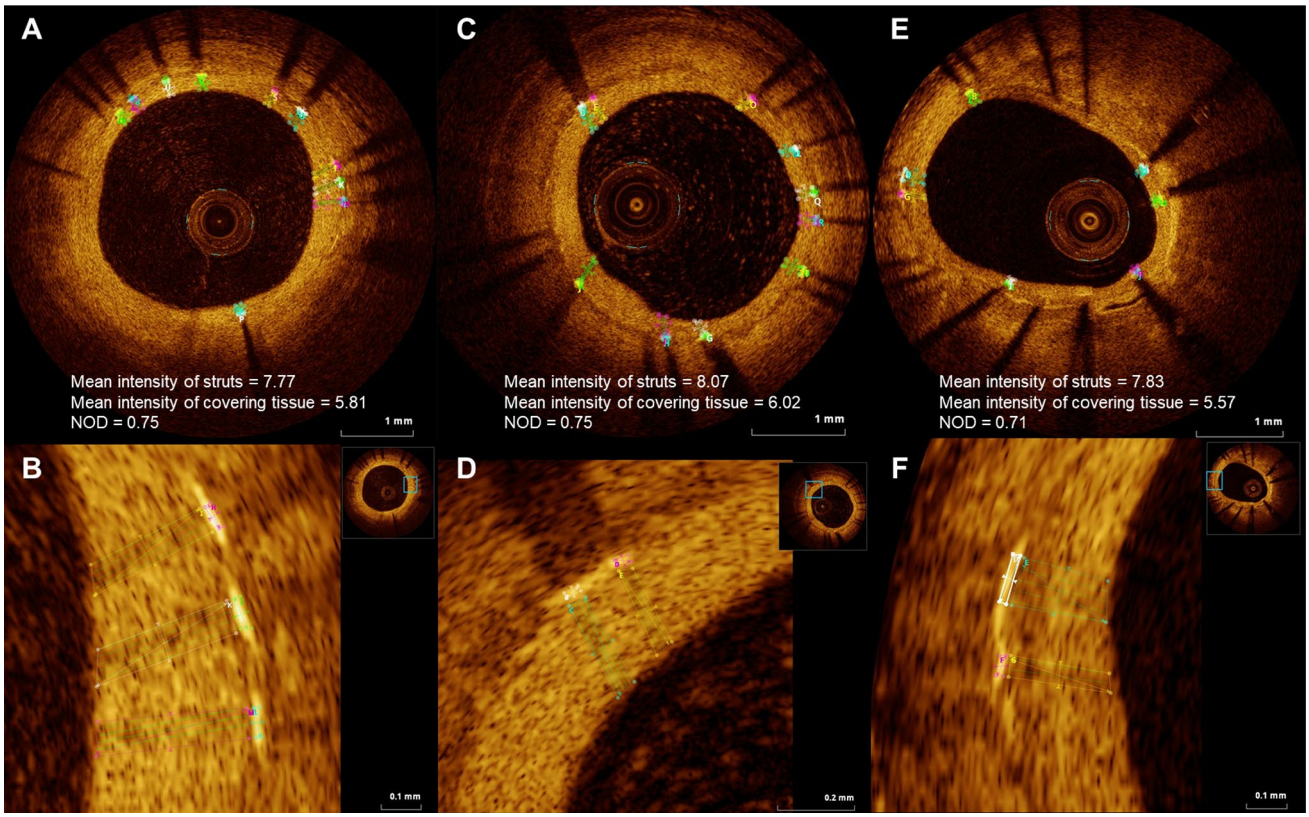

Fig. 4 Representative OCT cross-sectional images with NOD analysis for BMS (**a** and **b**), ZES (**c** and **d**) and EES (**e** and **f**) are shown. The methodology for calculation of NOD is described in Fig. 1

loss and neointimal thickening (i.e., restenosis) are the biological response to vascular injury characterized by a sequence of endothelial denudation, platelet deposition and inflammatory cell recruitment, smooth muscle cell migration and proliferation, and extracellular matrix deposition. Re-endothelialization and complete neointimal coverage of the stent struts are commonly viewed as markers of favorable vascular healing [2, 18]. Recently, characterization of tissue maturation after DES implantation has been recognized as an important step forward in the assessment of vascular healing. Histological analysis of regions of mature neointimal tissue showed significantly higher smooth muscle cells and, in turn, proteoglycan/collagen, fibrin and inflammatory cells. In contrast, immature neointimal tissue was predominantly composed of macrophages with minimally interspersed smooth muscle cells [11]. Thus, neointimal immaturity is potentially associated with development of neoatherosclerosis, the atherosclerotic change within neointima [19] that has been regarded as a primary mechanism of late-stent failure after DES implantation [20]. A similar incidence of neoatherosclerosis has been observed for both second-generation and first-generation DESs [21]. Tsujita et al. showed that intravascular ultrasound (IVUS)-derived necrotic and less-fibrotic neointimal formation were frequently observed in the site of DESs implantation using dedicated software [IVUS-based tissue characterization software: iMap (Boston Scientific, Natick, MA)]. The result of our study that NOD was lower at EES sites than at BMS and ZES sites suggests a potential risk for neoatherosclerosis at EES sites. These findings are consistent with previous reports.

We have been investigating the role of circulating bone marrow-derived progenitor cells on the biological response after stent deployment using translational research techniques that include both flow cytometry and OCT imaging. First, we demonstrated that mobilization of CD34+ increased from baseline during the acute phase (7–14 days) after BMS deployment, and was associated with late-lumen loss and restenosis at follow-up coronary angiography. The first-generation SES suppressed late-lumen loss and CD34+ cell mobilization, raising the question of whether neointimal suppression is inexorably linked with impaired re-endothelialization [2, 7]. Next, we observed that even second generation DESs, including ZESs and EESs, suppressed the mobilization of CD34+/CD133+/CD45low cells during the acute phase after stent deployment (on day 7) and inhibited subsequent neointimal formation. Furthermore, EES deployment was associated with an increased number of uncovered stent struts, compared with BMS deployment

[22]. Finally, we also performed a study in vitro to investigate the pharmacological action of the drugs coated on the surface of DESs on the differentiation of progenitor cells into vascular cells. The results showed that everolimus, zotarolimus and sirolimus all inhibited differentiation of progenitors into endothelial cell as well as smooth muscle cell-like lineages, indicating a drug class effect on progenitor cell differentiation [23]. These results strongly suggest that neointimal suppression utilizing DESs with -limus derivatives are biologically linked with impaired wound healing responses (i.e., re-endothelialization and incomplete stent strut coverage) as a consequence of reduced mobilization of stem cell progenitors, especially in the case of EESs. In the present study, we could not measure CD34+/CD133+/CD45low cells during the acute phase but did so at the time of follow-up coronary angiography. The percent change in the number of CD34+/CD133+/CD45low cells were less in the EES group than the BMS group. These results suggest the possibility that lower progenitor cell mobilization might be associated with neointimal immaturity in the EES lesions. We also measured serum levels of SDF-1α, IL-8 and MMP-9, all of which are considered to be related to mobilization of progenitor cells. Consequently, the NOD value was negatively correlated with the percent change in MMP-9 level. Since MMP-9 is a proteolytic enzyme that promotes matrix degradation and plays a pathophysiologic role in atherosclerotic plaque vulnerability and rupture, our results strongly suggest that MMP-9 contributes to neointimal immaturity in the vascular healing process after stent injury. Although DESs strongly inhibit the inflammatory reaction during the acute phase after stent implantation, there is impairment of the subsequent wound-healing response initiated by impaired re-endothelialization. This causes a relapse of inflammation, and inflammatory cells such as lymphocytes as well as macrophages play an essential role [6, 24–26]. The MMP-9 released from these cells possibly inhibits neointimal maturity, leading to impairment of vascular healing at the stented vessel sites.

Limitations and clinical implications

In the present study, we assessed NOD as a marker of neointimal maturity. The NOD was calculated based on the average neointima for all stent struts in the analyzed frames. We assessed the average neointimal maturity because we tried to perform quantitative assessment. However, tissue characteristics of neointima are heterogeneous, and our analysis did not include any histological validation. For example, collagen fiber-rich neointima exhibits stronger optical scattering and therefore a stronger OCT signal, whereas tissues made up of lipids, such as the necrotic core, appear as low-intensity areas with diffuse borders [27]. Therefore, detailed qualitative assessment for each type of neointima is needed. Despite the suitability of NOD assessment for vascular healing after stent implantation, this model remains hampered by its inability to reflect important patient comorbidities and other dependent parameters, such as the presence of risk factors and the influence of medications that may affect stent healing. Since the number of samples was limited, further studies are required to confirm the significance and application of our findings in a larger cohort. Despite a number of limitations, our results suggest that it is important to assess neointimal quality such as tissue characteristics in addition to neointimal growth in terms of physiological vessel wound healing after stent deployment.

Conclusions

Neointimal maturity might be lower at EES sites, compared with BMS and ZES sites. This might lead to impaired neointimal tissue growth, and might be associated with matrix degradation. These results suggest a specific pathophysiology after DES implantation.

Funding This work was supported in part by a Grant-in-Aid for Scientific Research from the Ministry of Education, Science and Culture of Japan (Grant No. 22590794) and by a Grant of the Vehicle Racing Commemorative Foundation, Tokyo, Japan (661).

Compliance with ethical standards

Conflict of interest The authors declare that they have no conflict of interest.

References

1. Rogers C, Parikh S, Scifert P et al (1996) Endogenous cell seeding: remnant endothelium after stenting enhances vascular repair. Circulation 94:2909–2914
2. Inoue T, Croce K, Morooka T et al (2011) Vascular inflammation and repair: implication for reendothelialization, restenosis, and stent thrombosis. J Am Coll Cardiol Intv 4:1057–1066
3. Farb A, Burke AP, Kolodgie FD et al (2003) Pathological mechanisms of fetal late coronary stent thrombosis in humans. Circulation 108:1701–1706
4. Alfonso F, Suárez A, Pérez-Vizcayno MJ et al (2007) Inravascular ultraaound findings during episodes of drug-eluting stent thrombosis. J Am Coll Cardiol 50:2095–2097
5. Cook S, Wenaweser P, Togni M et al (2007) Incomplete stent apposition and very late stent thrombosis after drug-eluting stent inplantation. Circulation 115:2426–2234
6. Taguchi I, Yoneda S, Abe S et al (2014) The late phase inflammatory response after drug-eluting stent implantation. Heart Vessels 29:213–219
7. Inoue T, Sata M, Hikichi Y et al (2007) Mobilization of CD34-positive bone marrow-derived stem cells after coronary stent implantation: impact on restenosis. Circulation 115:553–561

8. Templin C, Meyer M, Müller MF et al (2010) Coronary optical frequency domain imaging (OFDI) for in vivo evaluation of stent healing: comparison with light and electron microscopy. Eur Heart J 31:1792–1801
9. Attizzani GF, Bezerra HG, Chamié D et al (2012) Serial evaluation of vascular response after implantation of a new sirolimus-eluting stent with bioabsorbable polymer (MISTENT): an optical coherence tomography and histopathological study. J Invasive Cardiol 24:560–568
10. Attizzani GF, Bezerra HG, Ormiston J et al (2013) Serial assessment by optical coherence tomography of early and late vascular responses after implantation of an absorbable-coating sirolimus-eluting stent (from the first-in-human DESSOLVE I trial). Am J Cardiol 112:1557–1564
11. Malle C, Tada T, Steigerwald K et al (2013) Tissue characterization after drug-eluting stent implantation using optical coherence tomography. Arterioscler Thromb Vasc Biol 33:1376–1383
12. Bezerra HG, Costa MA, Guagliumi G et al (2009) Intracoronary optical coherence tomography: a comprehensive review clinical and research applications. J Am Coll Cardiol Intv 2:1035–1046
13. Guagliumi G, Gi Musumec, Sirbu V et al (2010) Optical coherence tomography assessment of in vivo vascular response after implantation of overlapping bare-metal and drug-eluting stents. J Am Coll Cardiol Intv 3:531–539
14. Mehanna EA, Attizzani GF, Kyono H et al (2011) Assessment of coronary stent by optical coherence tomography, methodology and definitions. Int J Cardiovasc Imaging 27:259–269
15. Umemura T, Soga J, Hidaka T et al (2008) Aging and hypertension are independent risk factors for reduced number of circulating endothelial progenitor cells. Am J Hypertens 21:1203–1209
16. Arao K, Yasu T, Ohmura N et al (2010) Circulating CD34+/CD133+ progenitor cells in patients with stable angina pectoris undergoing percutaneous coronary interventions. Circ J 74:1929–1935
17. Kereiakes DJ (2017) The TWENTE trial in perspective: stents and stent trials in evolution. JAMA Cardiol 2:235–237
18. Inoue T, Node K (2009) Molecular basis of restenosis and novel issues of drug-eluting stents. Circ J 73:615–621
19. Nakazawa G, Otsuka F, Nakano M et al (2011) The pathology of neoatherosclerosis in human coronary implants bare-metal and drug-eluting stents. J Am Coll Cardiol 57:1314–1322
20. Park SJ, Kang SJ, Virmani R et al (2012) In-stent neoatherosclerosis: a final common pathway of late stent failure. J Am Coll Cardiol 59:2051–2057
21. Lee SY, Hur SH, Lee SG et al (2015) Optical coherence tomographic observation of in-stent neoatherosclerosis in lesions with more than 50% neointimal area stenosis after second-generation drug-eluting stent implantation. Circ Cardiovasc Interv 8:e001878
22. Tsujita K, Takaoka N, Kaikita K et al (2013) Neointimal tissue component assessed by tissue characterization with 40 MHz intravascular ultrasound imaging: comparison of drug-eluting stents and bare-metal stents. Catheter Cardiovasc Interv 82(7):1068–1074
23. Sakuma M, Nasuno T, Abe S et al (2018) Mobilization of progenitor cells and assessment of vessel healing after second generation drug-eluting stenting by optical coherence tomography. Int J Cardiol Heart Vasc 18:17–24
24. Abe S, Yoneda S, Kanaya T et al (2012) Pathological features of in-stent restenosis after sirolimus-eluting stent vs bare metal stent placement. Cardiovasc Pathol 21:e19–e22
25. Yoneda S, Abe S, Taguchi I et al (2012) Inflammation and impaired wound healing after zotarolimus-eluting stent implantation. Cardiovasc Pathol 21:511–514
26. Yoneda S, Abe S, Kanaya T et al (2013) Late phase inflammatory response as a feature of in-stent restenosis after drug-eluting stent implantation. Coron Artery Dis 24:368–373
27. Shibuya M, Fujii K, Hao H et al (2015) Tissue characterization of in-stent neointima using optical coherence tomography in the late phase after bare-metal stent implantation—an ex vivo validation study. Circ J 79:2224–2230